Chapter 1
Introduction to Supramolecular Chemistry

1.1. General Overview

This chapter is intended to describe the principles, perspectives, and recent developments in the field of supramolecular chemistry, which has grown exponentially in the last few decades as indicated by the large number of articles, reviews, and books.[1-7] The emergence of supramolecular chemistry has had a profound effect on how efficiently chemists prepare structures of different sizes and shapes with dimension in the range of 1 to 100 nm using spontaneous secondary interactions such as hydrogen bonding, dipole-dipole, charge transfer, van der Waals, and π–π stacking interactions.[8-13] This so-called "bottom up" approach to construct nanostructures is advantageous over the "top down" approach such as microlithography which requires substantial effort to fabricate microstructures and devices as the target structures are extended to the range below 100 nm.[2]

Therefore, there is an increasing realization that the "bottom up" approach would open a route to nanostructures that are currently inaccessible by the "top down" approach. Thus far the development of the "bottom up" methods to create nanostructures have been inspired primarily by Nature, which displays a wide variety of complex nanostructures with astonishing precision.[14,15] These nanoscale structures in biological systems are specifically put together from two or more small molecular components by means of secondary interactions. The precision and specificity are indicative of control and directionality displayed by secondary interactions between complementary components in biological systems. In addition, the "bottom up" approach benefits from having thermodynamic minima in its resulting nanostructures due to the reversible nature of secondary interactions. Obviously, the challenge is to synthetically create nanostructures with such precision and specificity as seen in biological systems by cleverly incorporating complementary recognition sites in the molecular components for secondary interactions. This challenge is only met by first understanding how molecular

self-assembly in biological systems operates to generate well-defined aggregates and then transferring the knowledge learned from biological systems to chemical synthesis.

1.2. Self-Assembly in Nature

Naturally occurring DNA, perhaps the best known self-assembling structure in biological systems, exists in a double helical form.[16] The two single strands are held together by a number of hydrogen bonds, involving acidic hydrogen atoms (hydrogen bonding donor), oxygen (hydrogen bonding acceptor), and nitrogen atoms (hydrogen bonding acceptor) of the purine and pyrimidine bases in order to maintain the double helical structure (Figure 1.1a). In this double helix guanine (G) forms triple hydrogen bonds with cytosine (C) and adenine (A) forms double hydrogen bonds with thymine (T) (Figure 1.1b). Guanine selectively interacts with cytosine because the G-C complex is much more stable than G-T complex which would form only one hydrogen bond. Similarly, adenine exclusively complexes with thymine because adenine would form no hydrogen bonds with cytosine. The X-ray diffraction studies revealed that the hydrogen bonds holding G-C and A-T complexes are about the same length (2.9 ± 0.1 Å).

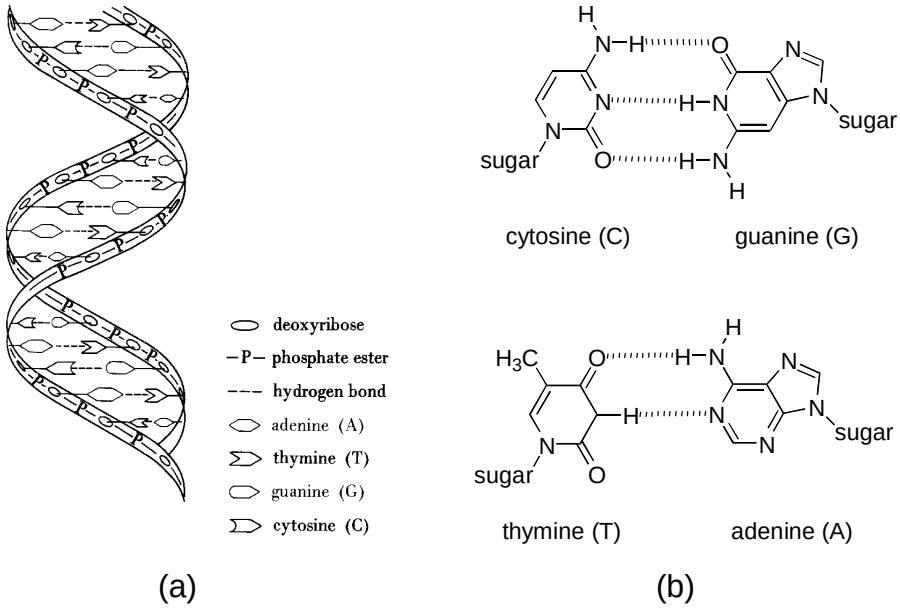

Figure 1.1. a) Complementary base pairing in DNA helical structure and b) base pairing in DNA (guanine and cytosine form triple hydrogen bonds; adenine and thymine form double hydrogen bonds).[17]

Another example of well-investigated and understood biologically existing nanostructures is the tobacco mosaic virus (TMV) (Figure 1.2).[2,4,14,18] TMV was the first virus to be discovered (by Demitri Iwanowsky in 1892) and isolated (by Wendell Stanley in 1935). This helical virus is a rod-shaped particle with dimensions of 300 nm in length and 18 nm in diameter, and has a particle mass of 4.0×10^7 daltons. A total of 2130 identical protein subunits, each with 158 amino acids, surround a single strand of RNA containing 6390 nucleotide bases to form this helical virus. First, protein subunits (17 or 18 subunits are required) form a stable doubly docked disk subassembly (Figure 1.3a) and an RNA strand is inserted into the central hole of the disk in such a way that the disk subassembly is transformed into two turns of a helical subassembly (Figure 1.3b). This helical subassembly is then cooperatively added to a growing helical assembly in an orderly arrangement at one or both ends of the helix (Figure 1.3c) and this process is repeated until the TMV nanostructure is complete (Figure 1.3d). The low probability of generating a defect TMV structure is attributed to the *in vitro* assembly process. In other words, the formation of a doubly docked disk subassembly from protein subunits is under thermodynamic control.

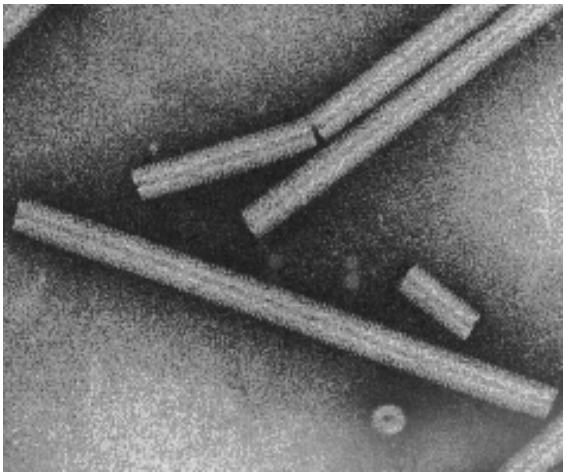

Figure 1.2. Electron micrograph of the tobacco mosaic virus.[18]

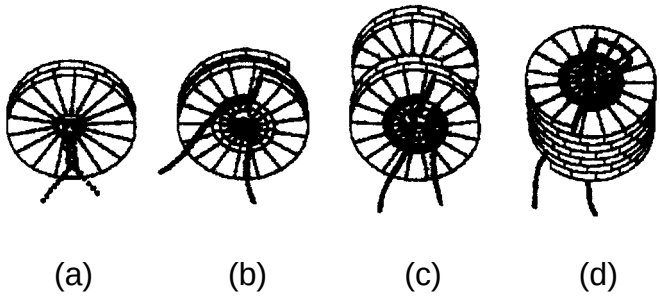

Figure 1.3. Self-assembly of the tobacco mosaic virus at different stages.[4]

Both the α-helix and the β-pleated sheet, derived from polypeptide chains depending on chain conformations, are other remarkable examples of how self-assembly is utilized to generate well-defined nanostructures in biological systems.[18] The α-helix is a rod-like structure of 0.5 nm diameter. This helix is stabilized by intramolecular hydrogen bonds involving the amide hydrogen (hydrogen bonding donor) and the carbonyl oxygen (hydrogen bonding acceptor). Figure 1.4 indicates that the hydrogen bonds are arranged such that the C=O group of the *n*th residue is perfectly situated for the interaction with the N-H group of the (n + 4)th residue. As a result nearly the optimum hydrogen bonding distance is observed for N-H···O=C (2.8 Å). It is noteworthy that all the N-H groups and C=O groups in the α-helix participate in hydrogen bonding. In addition, the core of the α-helix is tightly packed so that van der Waals interactions between the atoms situated in the core also stabilize the helix. The R groups point outward so as to avoid steric interference from the polypeptide backbone and from each other.

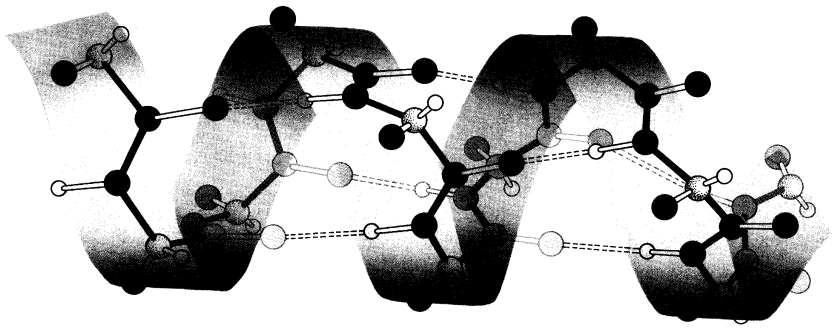

Figure 1.4. Model of α helix. Hydrogen bond interactions are denoted by dotted lines.[18]

In contrast, the β-pleated sheet, the other polypeptide secondary structure, is stabilized by intermolecular hydrogen bonding of N-H···O=C between neighboring polypeptide chains that are almost fully extended. Two types of the β-pleated sheets are realized, depending on the direction the neighboring polypeptide chains run. The neighboring chains run in opposite direction in the antiparallel β-pleated sheet (Figure 1.5a) while they run in the same direction in the parallel β-pleated sheet (Figure 1.5b).

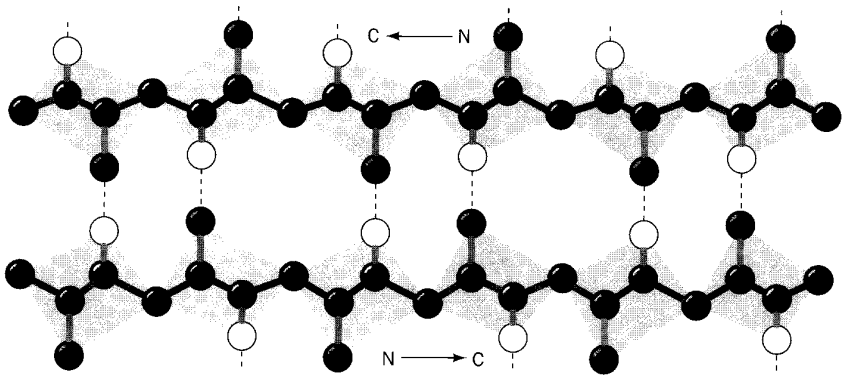

(a)

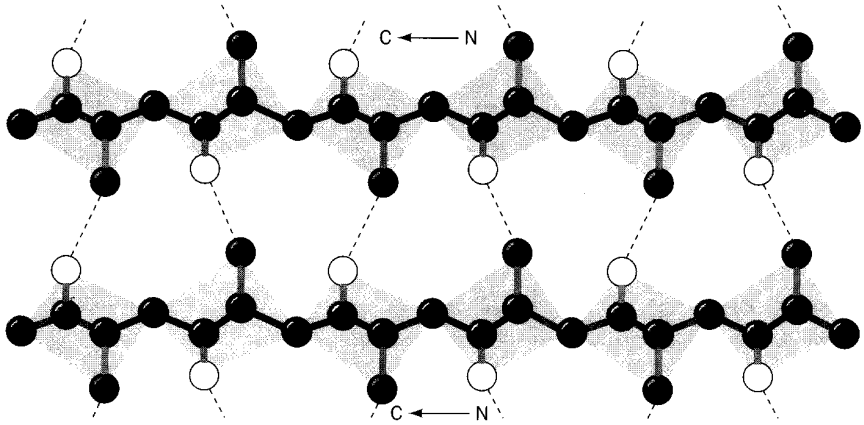

(b)

Figure 1.5. Models of β-pleated sheets. Side-chains are omitted for clarity. a) The antiparallel β-pleated sheet and b) the parallel β-pleated sheet. Hydrogen bonding interactions are denoted by dotted lines.[18]

1.3. Self-Assembly in Synthetic Chemistry

Over the last few decades many examples of supramolecular assemblies have been reported involving secondary interactions of hydrogen bonding, π-stacking, charge transfer, hydrophilic-hydrophobic, and chelation of metal cations. This section is devoted to describing the recent advances in the area of supramolecular chemistry which are divided into three different fields, namely organic, inorganic, and polymer chemistry.

1.3.1. Supramolecular organic chemistry

The two dimensional hydrogen bonded molecular network based on the secondary interactions between cyanuric acid and melamine was first reported by Wang and his coworkers in 1990 by resolving the crystal structure obtained from HCl solution (Figure 1.6).[19] Whitesides and his coworkers then successfully capitalized on this discovery by constructing roughly a globular nanostructure from cyanuric acid **1** and melamine derivatives **2**.[2,20,21] Their approach to the well-defined molecular globular structure is illustrated in Figure 1.7. To overcome a large entropy penalty associated with bringing 12 molecules into one aggregate, two cyanuric acid units and three melamine units were preorganized by covalently connecting them with rigid spacers so as to situate them in appropriate positions for optimum hydrogen bonding interactions. The 2:3 complex **3** was quantitatively formed in chloroform-*d*. It should be noted that when flexible spacers were used the target aggregate was not observed in solution, presumably due to the entropic cost of freezing conformational freedom in the flexible spacers.

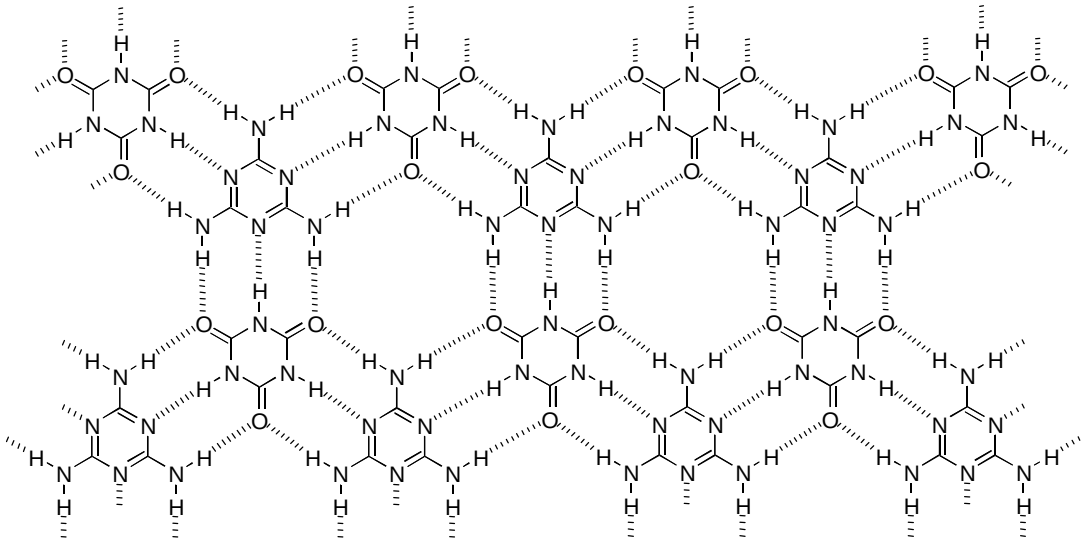

Figure 1.6. The crystal structure of the 1:1 complex of cyanuric acid and melamine.[19]

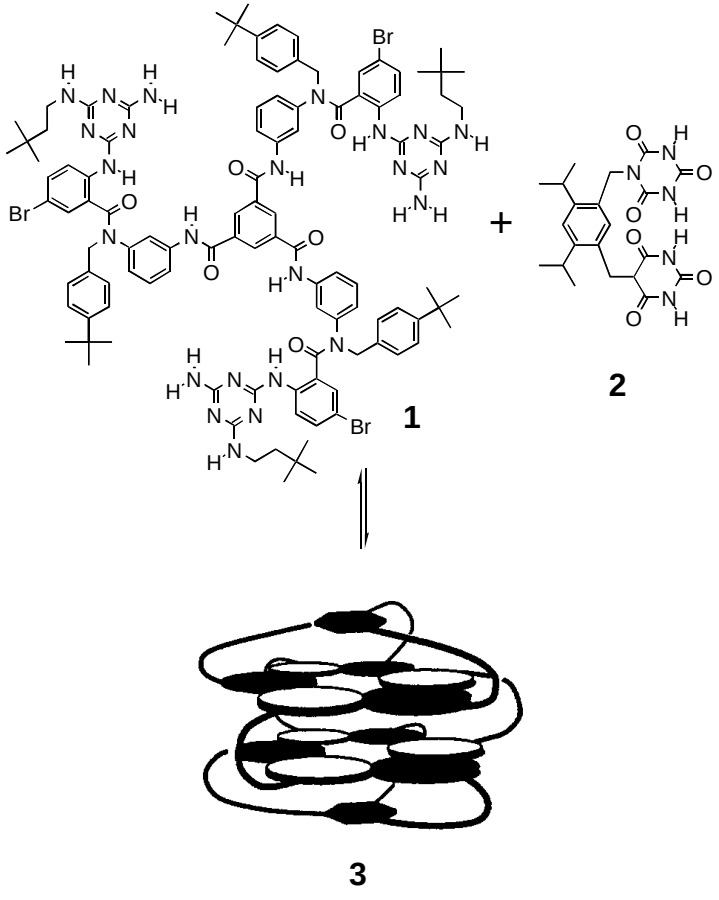

Figure 1.7. Complex **3** formed from **1** and **2**.[20]

More recently Whitesides and his coworkers introduced a semiquantitative method for predicting all entropic costs (translational, rotational, conformational, and vibrational entropy) in multiparticle assembly such as their molecular self-assembling structures based on the cyanuric acid-melamine hydrogen bonding interaction.[22] The model molecular structures used for this study are represented in Figure 1.8. For example, the contribution of conformational entropy for the formation of complex **5** was determined by simply subtracting the free energy of assembly for complex **4** from that for complex **5**. The conformational entropy for **6** was estimated similarly. Although this method is just an approximation, it is conceptually useful for evaluating entropy contributions based on geometric shapes of multiparticle molecular assemblies.

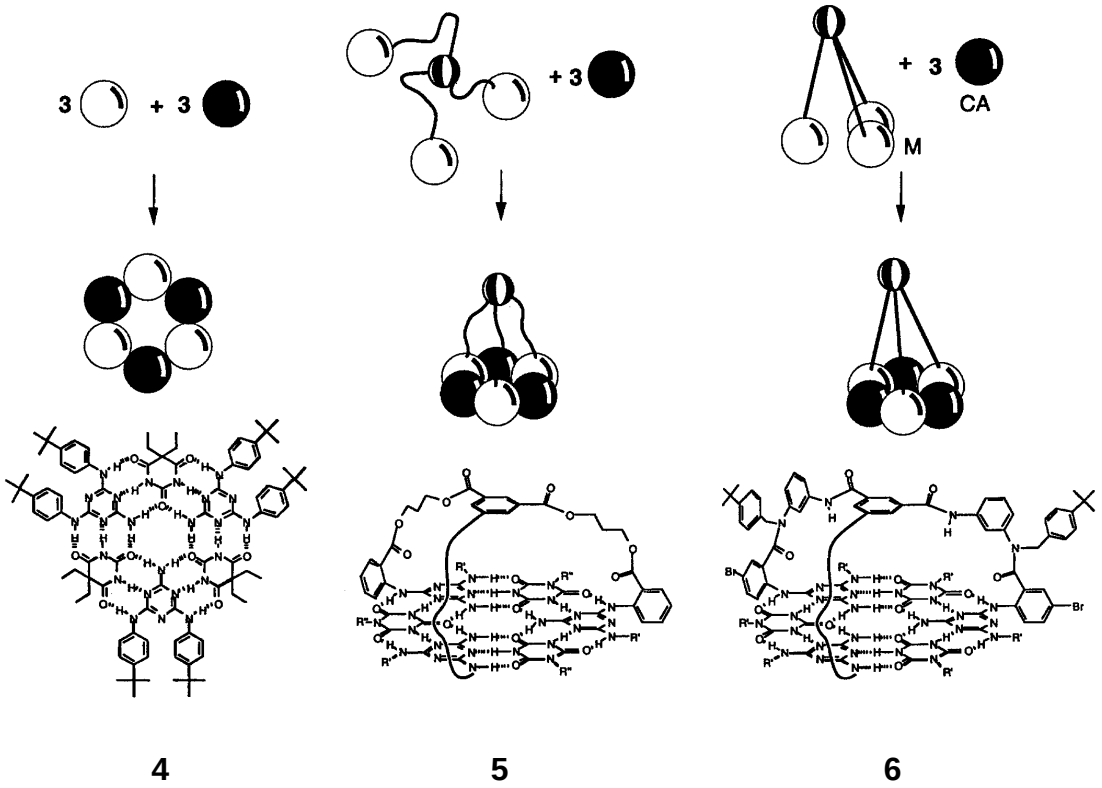

Figure 1.8. Molecular structures of **4**, **5**, and **6** and their cartoon representations using balls, strings, and rods. Black and white balls denote melamine and cyanuric acid units, respectively. Strings and rods denote flexible and rigid bridging units, respectively.[22]

The concept of molecular recognition was extended by Rebek and his coworkers to construct stable dimeric complexes of self-complementary bisglycoluril subunits

which show curvature along the molecules, caused by the seven membered rings on both sides of the central benzene ring (their simplest bisglycoluril subunit **7** is shown in Figure 1.9).[8,23-26] All the hydrogen bonding sites are required to be on the same side of the molecule (U-shape conformation) in order to dimerize by 8 hydrogen bonding interactions. This dimeric species is remarkably stable and is capable of encapsulating single guest molecule, *e.g.*, methane and ethane, in its internal void as evidenced by ^{1}H NMR spectroscopy. In addition, the bisglycoluril molecule **8** (Figure 1.9) can catalyze a Diels-Alder reaction of *p*-benzoquinone and a thiophene dioxide derivative in *p*-xylene-d_{10}. The rate of the reaction was substantially accelerated in the presence of the dimeric capsule.

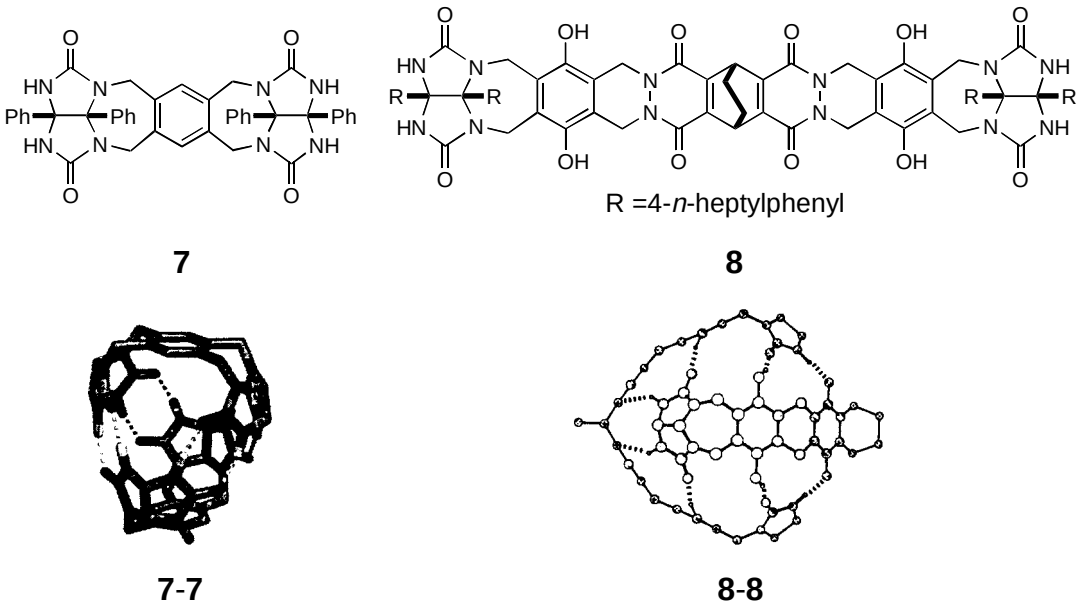

Figure 1.9. Molecular structures of **7** and **8** and the X-ray structures of the corresponding dimers **7**-**7** and **8**-**8**. Hydrogen bondings are denoted by dotted lines.[24,25]

Lehn and his coworkers employed a hydrogen bonding pattern method without the use of steric effects to enforce the outcome of the assembly to be a cyclic hexamer and not linear counterparts.[27] They cleverly designed and synthesized a pair of two-faced molecules **9** and **10** having two hydrogen bonding patterns to exclusively generate the cyclic hexamer entities **11** (Figure 1.10). Vapor pressure osmometry (VPO) and gel permeation chromatography (GPC) provided evidence for the cyclic aggregate formation.

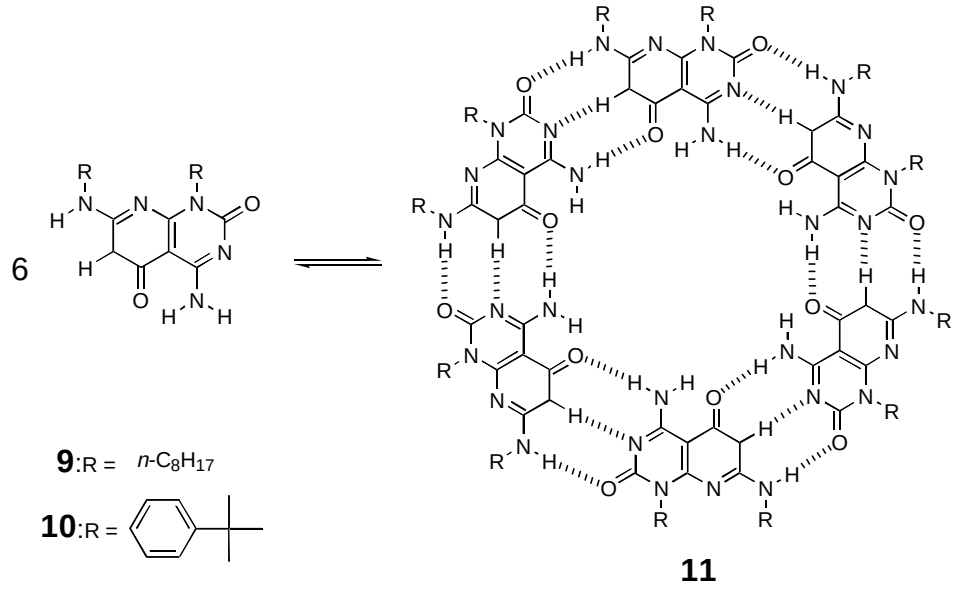

Figure 1.10. Structural representation of the cyclic hexamers **11** assembled from **9** and **10**.[27]

Stoddart's discovery that 4,4'-bispyridinium salts (paraquats) thread through the cavity of bis-*p*-phenylene-34-crown-10 (BPP34C10) to form pseudorotaxanes primarily based on C-H···O hydrogen bonding and electrostatic interaction between the π-electron-rich hydroquinol units and π-electron-deficient paraquat units stands as one landmarks of the chemistry of complexing crown ethers.[10,28-34] An immediate color change (from colorless to orange) upon mixing of equimolar solutions is indicative of charge transfer interaction. The X-ray structure of the pseudorotaxane **14** formed between BPP34C10 (**12**) and bismethylparaquat (**13**) revealed those interactions (Figure 1.11). At room temperature the ^{1}H NMR spectrum of equimolar solution of **12** and **13** (1.0×10^{-2} M each in acetone-d_6) revealed one set of signals, indicating that the rates of complexation and decomplexation are slow on the ^{1}H NMR time scale. This spectroscopic observation is not too surprising since the paraquat unit experiences no difficulties penetrating through the cavity of the crown ether. The association constant for the 1:1 complex **14** was determined to be 760 M^{-1} in acetone-d_6 at 25°C.

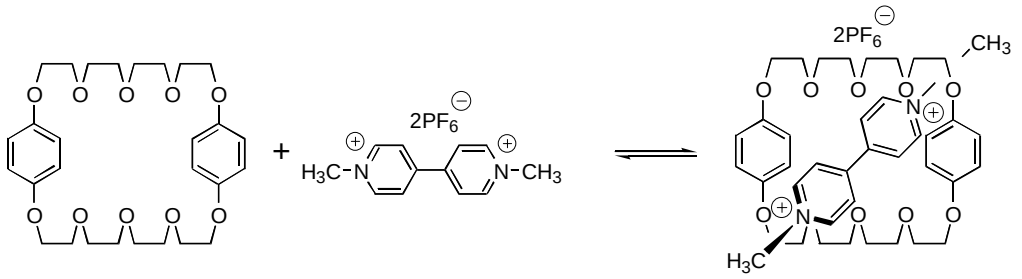

Figure 1.11. Formation of the pseudorotaxane **14** between **12** and **13**.[30]

The pseudorotaxanes based on dienzo-24-crown-8 (DB24C8) and secondary ammonium salts were also beautifully demonstrated by Stoddart and his coworkers. Figure 1.12 illustrates the formation of pseudorotaxane **17** between DB24C8 (**15**) and dibenzylammonium hexafluorophosphate (**16**).[11,34-50] In chloroform otherwise insoluble **16** becomes completely soluble upon addition of a stoichiometric amount of **15** due to the formation of the more soluble pseudorotaxane. Unlike the previous systems of BPP34C10 and paraquats, the ^{1}H NMR spectrum of equimolar solution of **15** and **16** (1.0 x 10^{-2} M each in acetone-d_6 at 25^{o}C) reveals three sets of signals corresponding to free crown ether, free salt, and 1:1 complex based on the argument of slow exchange on the ^{1}H NMR time scale. Indeed, CPK molecular modeling showed that the benzene ring of the salt had difficulties threading through the cavity of the crown ether. As for other self-assembling systems, the association constant was the highest in noncompetitive solvents and was estimated to be 2.7x10^4 M^{-1} in chloroform-*d* at 25°C. The X-ray structure of **17** shows hydrogen bonding interactions between -NH_2^+- and the oxygen atoms of the ethyleneoxy units of **15**. As observed for the pseudorotaxane **14**, π-stacking of one of somewhat electron deficient benzene rings of **16** and the electron rich catechol unit of **15** provides additional stabilization. This 1:1 complex was also observed in the gas phase using the soft ionization of fast atom bombardment (FAB) mass spectrometry, which minimizes the fragmentation of supramolecular assemblies.

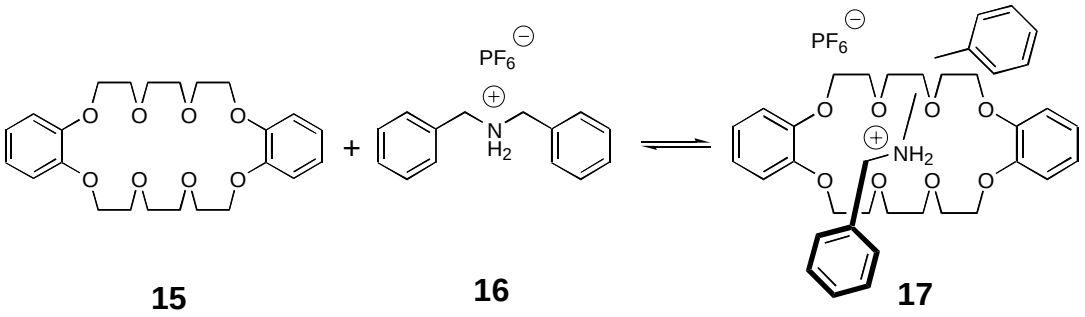

15 **16** **17**

Figure 1.12. Formation of the pseudorotaxane **17** between **15** and **16**.[41]

Loeb and his coworkers showed that the pseudorotaxane **19** between a newly designed bispyridinium salt, 1,2-bis(4,4'-dipyridinium)ethane dication (**18**), and **15** has improved stability by optimizing C-H···O hydrogen bonds (Figure 1.13).[51,52] The X-ray structure of the pseudorotaxane complex revealed that the complex is stabilized by eight C-H···O hydrogen bonds (only one C-H···O and two N^+-H···O hydrogen bonds were observed in the Stoddart's analog **14**). The association constant estimated for bispyridinium salt **18** and DB24C8 (**15**) in acetonitrile-d_3 displayed almost a three-fold increase compared to the Stoddart's analogous system.

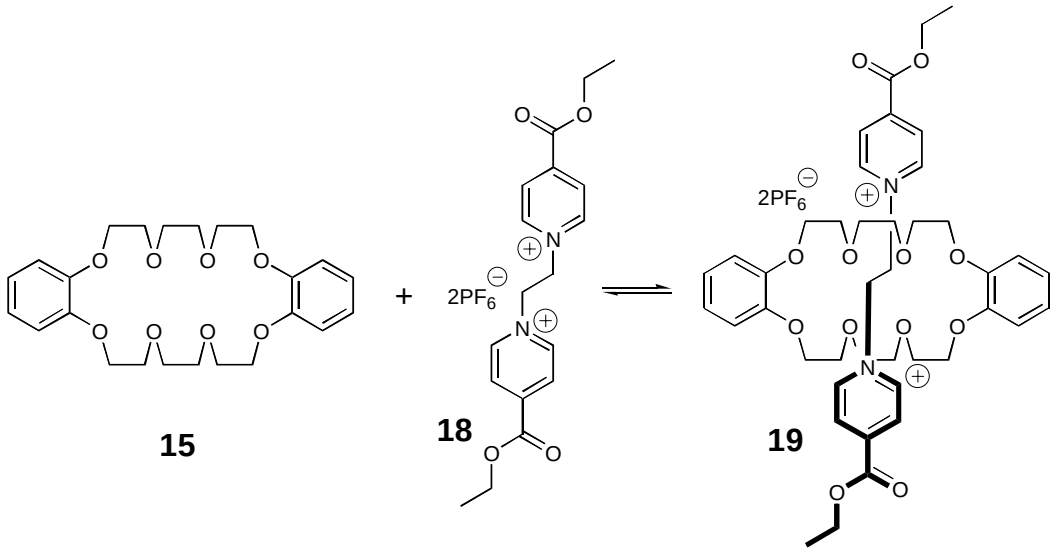

15 **18** **19**

Figure 1.13. Formation of the pseudorotaxane **19** between **15** and **18**.[52]

The most recent advance in pseudorotaxane synthesis was demonstrated by Sanders and his coworkers using bis(naphtho) crown ether **20** and diimide **21** (Figure 1.14).[53,54] Donor-acceptor interactions of the neutral aromatic units facilitate stable pseudorotaxane formation **22**. An immediate orange color was observed when equimolar dimethylformamide (DMF) solutions of the two components were mixed, indicating charge transfer interactions between the electron rich naphthols and the electron poor central benzene ring of the diimide unit. Such assemblies were remarkably stable and utilized as templates for the subsequent syntheses of neutral catenanes in good yields.

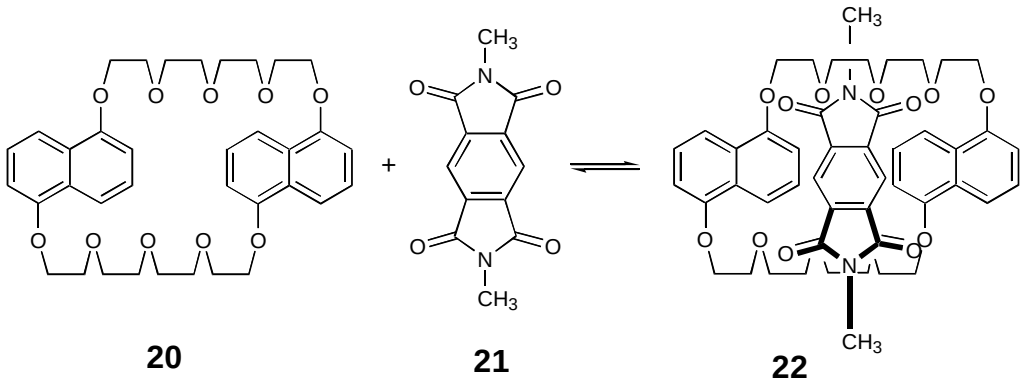

Figure 1.14. Formation of the psuedorotaxane **22** between **20** and **21**.[54]

1.3.2. Supramolecular inorganic chemistry

Supramolecular nanostructures can be constructed efficiently from organic ligands and metal ions as demonstrated by Sauvage and his coworkers.[55-58] In their pioneering work, the complex **24** formed between two 2,9-disubstituted 1,10-phenanthroline ligands **23** and copper(I) ion with tetrahedral coordination geometry indicates that the phenolic groups of two perpendicularly coordinating ligands point away from each other. This geometrical orientation of the functional groups favors the formation of the corresponding catenane (**25** in Figure 1.15).

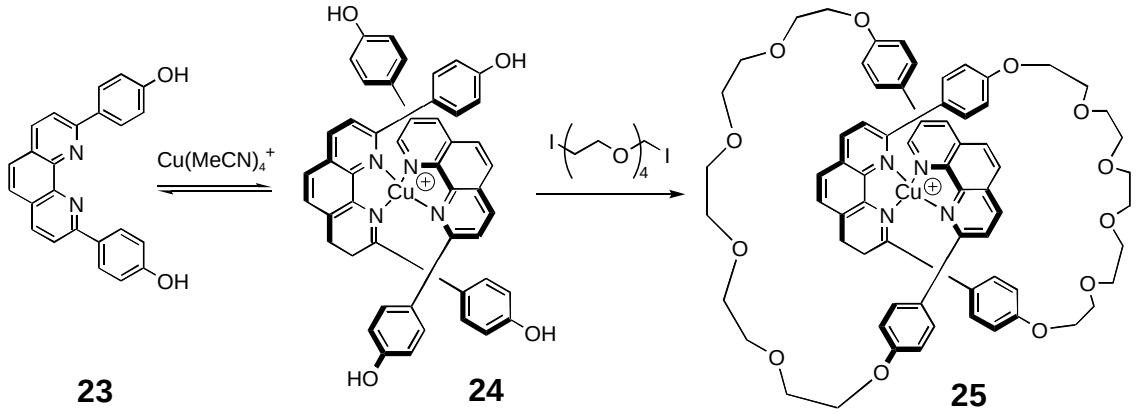

23 **24** **25**

Figure 1.15. Metal directed synthesis of the catenane **25**.[10]

The synthesis of a molecular knot was also made possible by the metal-ligand coordination method in the laboratories of Sauvage.[59,60] The double helical complex **27** formed between two bisphenanthroline ligands **26** and two copper(I) ions was subject to catenation with hexa(ethylene glycol) to yield the biscopper(I) of the knotted system (**28** in Figure 1.16) in 3% yield. The low yield was blamed on the flexible methylene spacer segment which increased the entropic penalty for the formation of the molecular knot. Indeed, when the flexible spacer was replaced with a rigid 1,3-phenylene in the bisphenanthroline ligand, the corresponding knotted product was generated in a remarkable 30% yield.

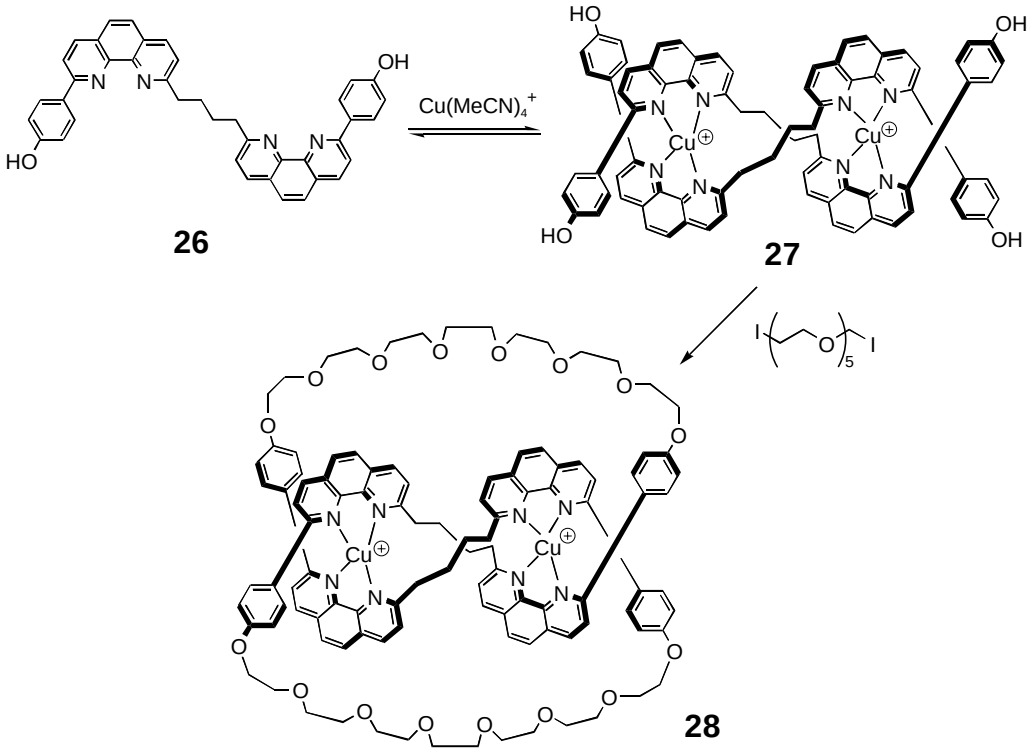

Figure 1.16. Metal directed synthesis of the molecular knot **28**.[10]

Fujita and his coworkers have also exploited metal coordination in the synthesis of nanosized structures using different metals such as palladium and platinum.[61,62] Their most recent achievement is the synthesis of a macrotricyclic nanostructure derived from ten small molecular components. The reactions of $[Pd(NO_3)_2(en)]$ (**29**) with a triazine-based ligand **30** in an aqueous solution afforded the macrotricyclic structure **31** in a remarkable 81% yield. This nanocage was demonstrated to trap two molecules of 4,4'-dimethylazobenzene in the internal void where they were shown to dimerize in the *cis*-conformation.

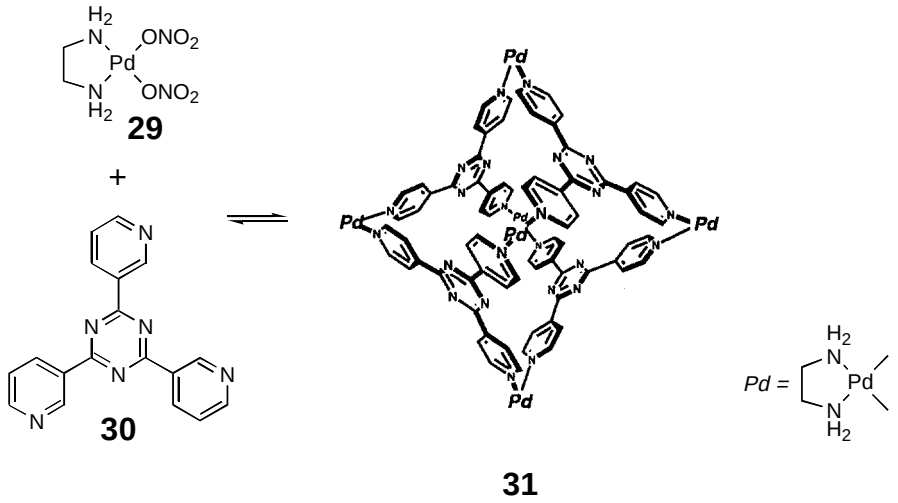

Figure 1.17. Synthesis of the nanocage **31**.[62]

Capitalizing on Fujita's breakthrough with the metal coordination approach to create supramolecular structures, Stang and his coworkers described the quantitative construction of well-defined molecular squares.[63-65] They have extended the concept of metal coordination to generate many nanosized polygon structures by varying the shape and length of organic ligand and connecting angle of metal.[66,67]

Combining the methods developed by Fujita, Stang, and others, Kim and his coworkers employed pseudorotaxane-type subunits of $[Pd(NO_3)_2(en)]$ (**29**), cucurbituril **32**, and *N*,*N*'-bis(4-pyridylmethyl)1,4-diaminobutane (**33**) to assemble the molecular necklace **34** in 90% yield (Figure 1.18).[68] The X-ray structure showed that every bispyridyl subunit was encircled by bead-like subunit of cucurbituril. The same approach was used to efficiently synthesize a molecular necklace with longer "string" and more "beads" threaded.

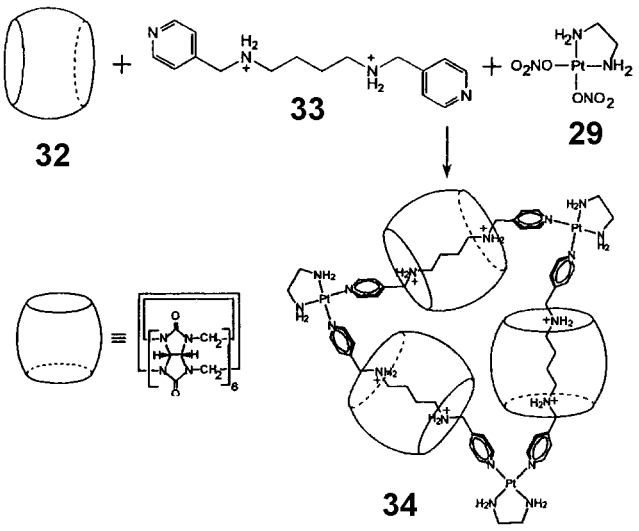

Figure 1.18. Synthesis of the molecular necklace **34**.[68]

1.3.3. Supramolecular polymer chemistry

Recently, Zimmerman and his coworkers introduced a self-assembly approach to dendrimer synthesis, which guarantees structural accuracy while eliminating steps from the conventional multistep approach, *i.e.*, convergent, divergent and double-stage convergent.[69,70] They prepared self-complementary subunits in which a series of Fréchet-Hawker type dendron units are covalently attached to an aromatic bridge bearing two isophthalic acid units (the fourth generation **35** is shown in Figure 1.19) and self-assembled them into cyclic hexamers in halogenated solvents, *e.g.*, chloroform and methylene chloride. The fourth generation self-assembling dendrimer **36** as shown in Figure 1.19 is disk-shaped with dimensions of 9 nm in diameter and 2 nm in thickness and its molecular mass almost reaches 35,000 g/mol. These dendritic species were characterized by vapor pressure osmometry (VPO), laser light scattering (LLS), and gel permeation chromatography (GPC) due to their remarkable stability in solution. The observed molecular weights showed good agreement with the theoretically calculated molecular weights for the hexameric aggregates. Although qualitative, ^{1}H NMR spectroscopy indicated the aggregation of the isophthalic acid units in chloroform-*d*.

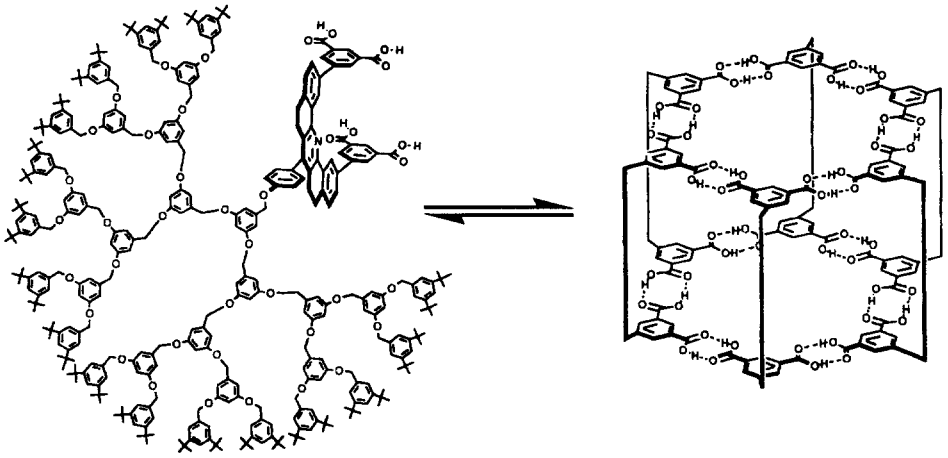

35 **36**

Figure 1.19. Synthesis of the fourth generation self-assembling dendrimer **36** from six units of **35**. The dendron wedges in **36** are omitted for clarity.[70]

Ghadiri and his coworkers successfully applied the knowledge learned from the β-pleated sheet, formed by intermolecular hydrogen bonding of neighboring polypeptide chains, to construction of a series of cyclic peptide nanotubes.[71-75] Cyclic peptides with alternating *D* and *L* amino acids in their cyclic chains **37** stack on top of one another by N-H···O=C intermolecular hydrogen bonding to form cylindrical structures **38** (Figure 1.20). Transport of glucose through these nanotubes was demonstrated. The size of internal pores of these self-assembling nanotubes are easily tuned by employing different ring sizes of cyclic peptides. To date, cyclic peptide nanotubes with internal diameter in the range of 0.7 to 1.3 nm have been constructed. In addition, the outside surface properties of these nanotubes can be altered by introducing different amino acid side chain groups, depending on their ultimate applications.

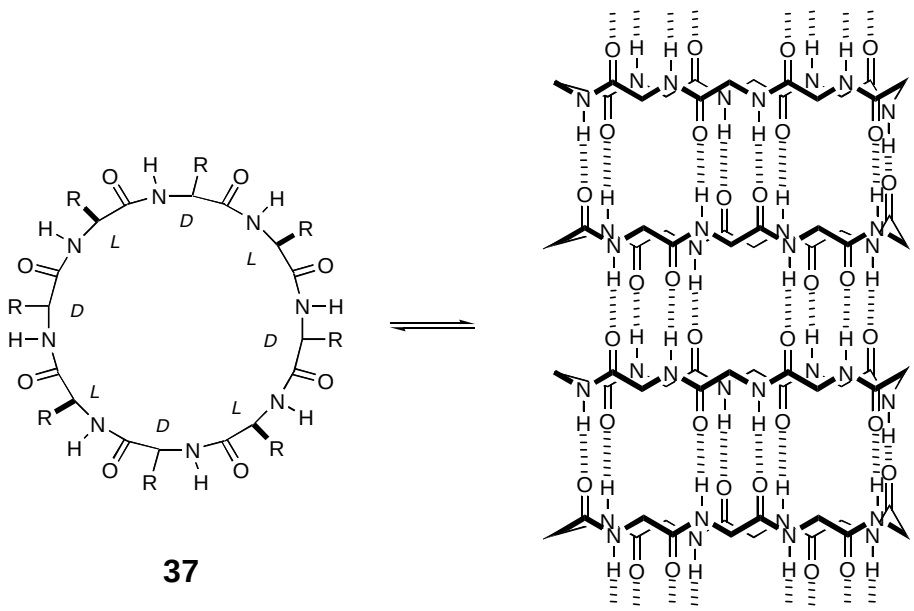

37 **38**

Figure 1.20. Construction of nanotubes **38** from cyclic peptides **37**.[74]

Gibson and his coworkers reported successful synthesis of main-chain polypseudorotaxanes **41** based on poly(ester-32-crown-10) **39** and *N*,*N*'-dialkyl-4,4'-bipyridinium salts (paraquats) (**40**) by taking advantage of the enthalpic driving forces of hydrogen bonding and electrostatic interaction (Figure 1.21).[76,77] The association constant (K_a) was significantly lower than the monomeric model system (60 vs. 250 M^{-1} in acetone-d_6 at 22°C) largely due to lack of preorganization of the crown ether receptors incorporated in the polymeric system. In solution the equilibrium of threading and dethreading was shifted right by either lowering the solution temperature or saturating the solution with paraquat. The viscosity measurements indicated an increased hydrodynamic volume as *m*/*n* values were increased due to pseudorotaxane formation. Solid-state samples of the polypseudorotaxanes with varied *m*/*n* values prepared by freeze-drying technique allowed the possibility of studies on their properties. Physical properties of the main-chain polypseudorotaxanes were shown to be tunable by adjusting the fraction of the crown ether receptors threaded with paraquat. In general, solubility of the polypseudorotaxanes was substantially improved as *m*/*n* values were increased

compared to those of the individual components. In addition, higher T_g's were recorded for polypseudorotaxanes with greater m/n values.

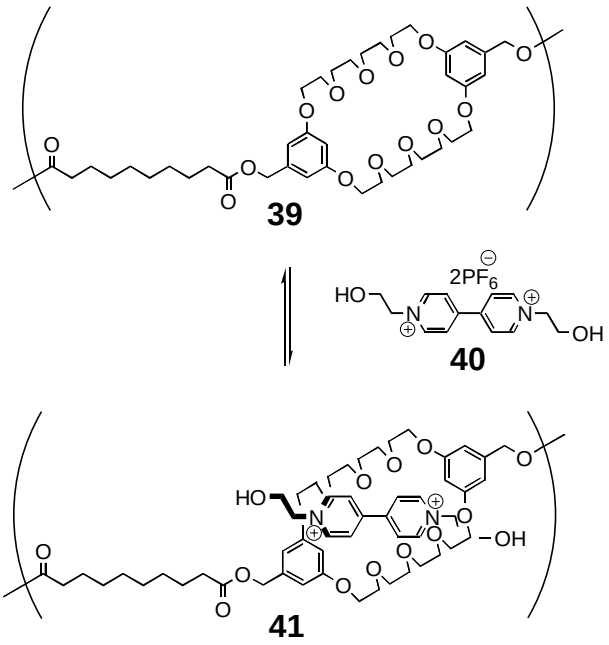

Figure 1.21. Synthesis of the main-chain polypseudorotaxane **41**.[77]

Main-chain polypseudorotaxanes **44** from linear polymers containing aromatic guest units **42** and a tetracationic cyclophane host **43** with two paraquat units have also been reported by Gibson, Hodge, and others (one representative structure from Hodge's work is shown in Figure 1.22).[78-81] The threading process is driven by π-stacking interaction between the electron-rich aromatic units of linear polymers and the electron deficient paraquat units of cyclophane along with charge transfer and hydrogen bonding interactions. In the systems of Hodge,[78] the K_a values were lower than those of the model systems by a factor of up to 2, and site occupancy was limited to 50-94%, depending upon the spacer length between guest sites in the polymer and the temperature. The remarkable efficiency (m/n =0.94) demonstrated in their systems despite potential electrostatic repulsion experienced by the adjacent cyclophane units was made possible by strong enthalpic forces.

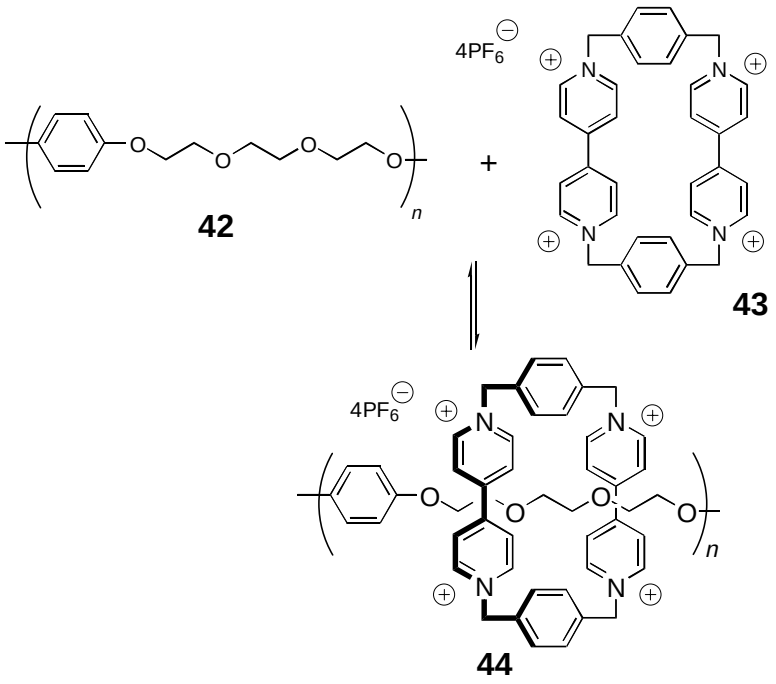

Figure 1.22. Synthesis of the main-chain polypseudorotaxane **44**.[78]

Swager and his coworkers synthesized polythiophenes and poly(phenyleneethynylene) containing crown ether receptors that are capable of forming side-chain polypseudorotaxanes with paraquat as sensory materials.[82,83]

Lehn and his coworkers took on a task of controlling the architecture of nanostructures as they build up from molecular components by self-assembly.[3,84-88] Spontaneous association of two complementary homoditopic components **45** and **46**, P and U (P stand for 2,6-diaminopyridine and U stands for uracil), with derivatives of *L*-, *D*-, and *meso*-tartaric acid spacer segments led to the formation of liquid crystalline suparmolecular polymers **47** through triple hydrogen bonding as shown in Figure 1.23.[3,87] This polymolecular entity showed entirely different thermal behavior from the individual homoditopic molecules. Thermotropic mesophases were observed for the mixtures (*L*P + *L*U), (*D*P + *L*U), and (*m*P + *m*U) from below room temperature to 220-250^{o}C, whereas the homoditopic molecules were crystalline solids. In order to obtain more information on microscale structural features, electron microscopy of these structures was performed. The mixture (*L*P + *L*U) yielded right-handed helical species (Figure 1.24a), while (*D*P + *D*U) gave left-handed helical structures (Figure 1.24b). It is

believed that the chirality placed in the spacer segment of the homoditopic molecules induce their helicity on the microscopic level. The mixture (*m*P + *m*U) did not induce helicity (Figure 1.24c).

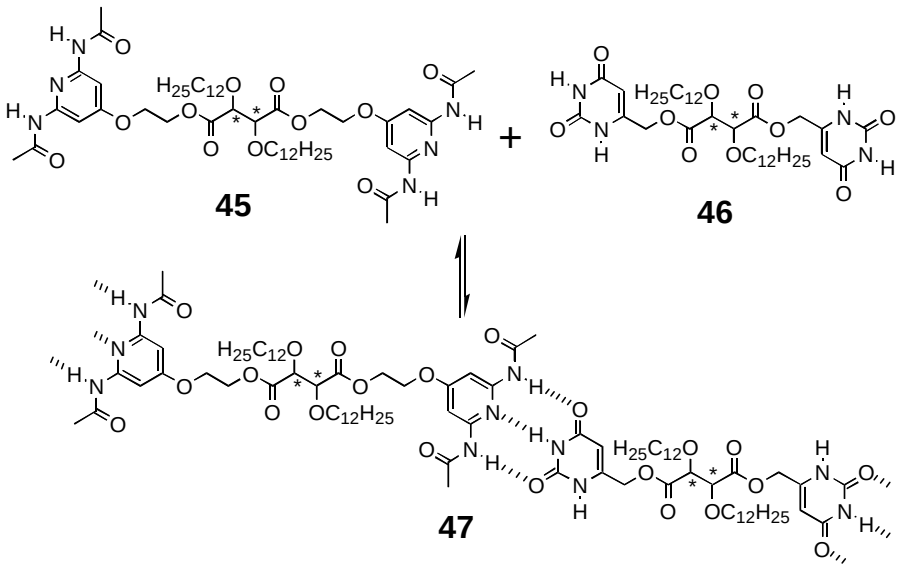

Figure 1.23. Self-assembly of thermotropic liquid crystalline polymers **47**.[87]

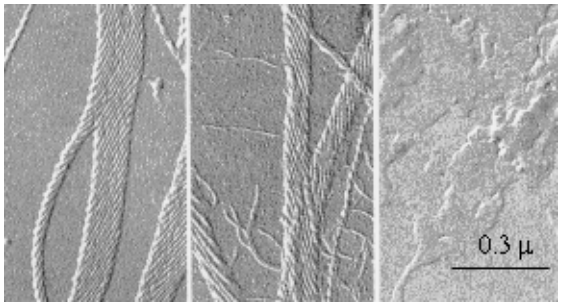

Figure 1.24. Electron micrographs of supramolecular polymers from the mixture a) *L*P + *L*U, b) *D*P + *D*U, and c) *m*P + *m*U.[87]

Lehn and his coworkers extended this concept further by incorporating a rigid rod spacer segment between the complementary units of homoditopic molecules **48** and **49** which were subsequently mixed (1:1 ratio) to form a lyotropic liquid crystalline polymeric structure **50** through triple hydrogen bondings (Figure 1.25).[3,87,88]

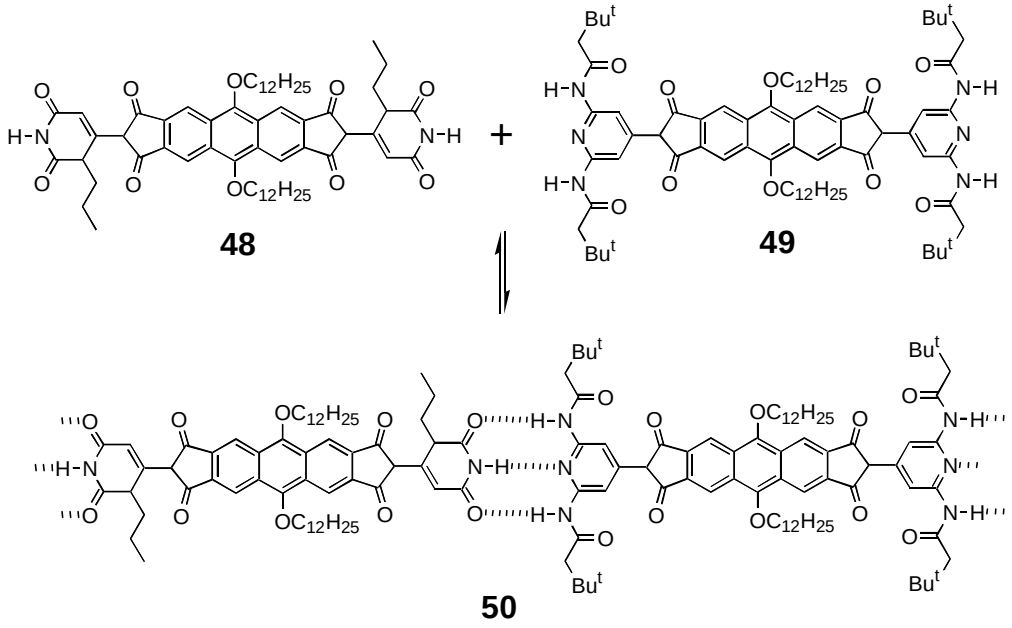

Figure 1.25. Self-assembly of lyotropic liquid crystalline polymer **50**.[87]

Kato and his coworkers have investigated analogous liquid crystalline supramolecular structures using preformed polymers that are capable of coupling with mesogenic groups by secondary interactions.[89-94] As an example, poly[4-(6-(acryloyloxy)hexyloxy)benzoic acid] (**51**), a polyacrylate bearing carboxylic acid groups, undergoes hydrogen bonding interaction with the pyridine unit of *trans*-4-alkoxy-4'-stilbazole (**52**) to form novel side-chain liquid crystalline polymer **53** (Figure 1.26).[93] The major advantage of these side-chain systems over Lehn's linear-chain systems is that the properties are readily tunable by simply coupling the preformed polymer with various mesogenic groups.

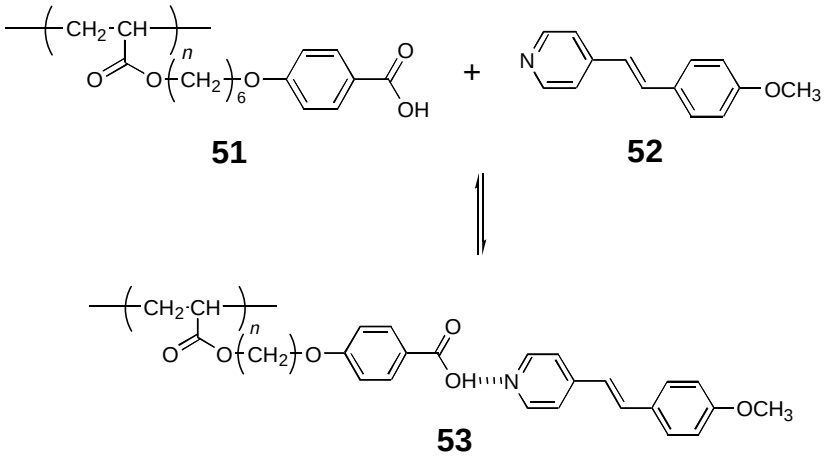

Figure 1.26. Self-assembly of side-chain liquid crystalline polymer **53**.[93]

Griffin and his coworkers have investigated on the use of tetrapyridyl unit **54** and diacid unit **55** en route to supramolecular polymeric network **56** and/or ladder structures **57** by means of hydrogen bonding (Figure 1.27).[95] This supramolecular network and/or ladder is thermally reversible, meaning that it behaves like polymeric materials at lower temperatures and shows characteristics of small molecules at higher temperatures. Fibers pulled from the melt are indicative of highly extended hydrogen bonding supramolecular structures.

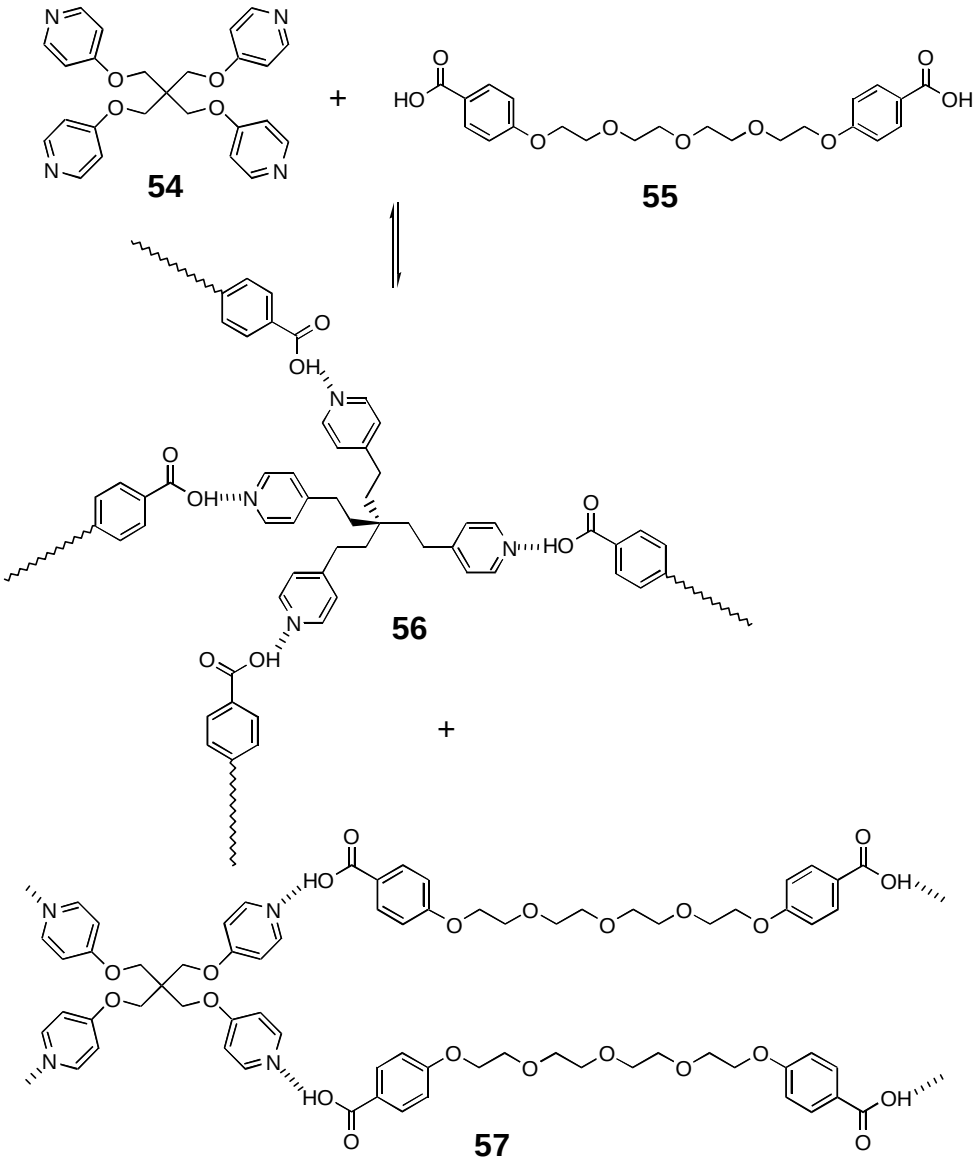

Figure 1.27. Self-assembly of polymeric network **56** and ladder structures **57**.[95]

In the laboratories of Meijer, the discovery of a significantly strong hydrogen bonding moiety based on the ureido-pyrimidone unit which is capable of dimerizing through a quadruple hydrogen bonding prompted them to utilize this unit as the complementary end group in supramolecular polymeric structures. The association constant (K_a) for dimerization of the ureido-pyrimidone is estimated to exceed 10^6 M^{-1} in chloroform at ambient temperature. Because of strong association of the quadruple hydrogen bonding, corresponding supramolecular polymers are expected to possess

comparable physical properties to the conventional covalent polymers.[96-98] To date, they have investigated two linear supramolecular polymers **59** and **61** formed from homoditopic molecules with the ureido-pyrimidone unit at both ends of hexamethylene and poly(dimethylsiloxane) (M_n = 8,000 g/mol) spacers, *i.e.*, **58** and **60**, respectively, as shown in Figure 1.28. Significant increases in solution viscosity at higher concentrations were reported for both of the self-assembling polymers.

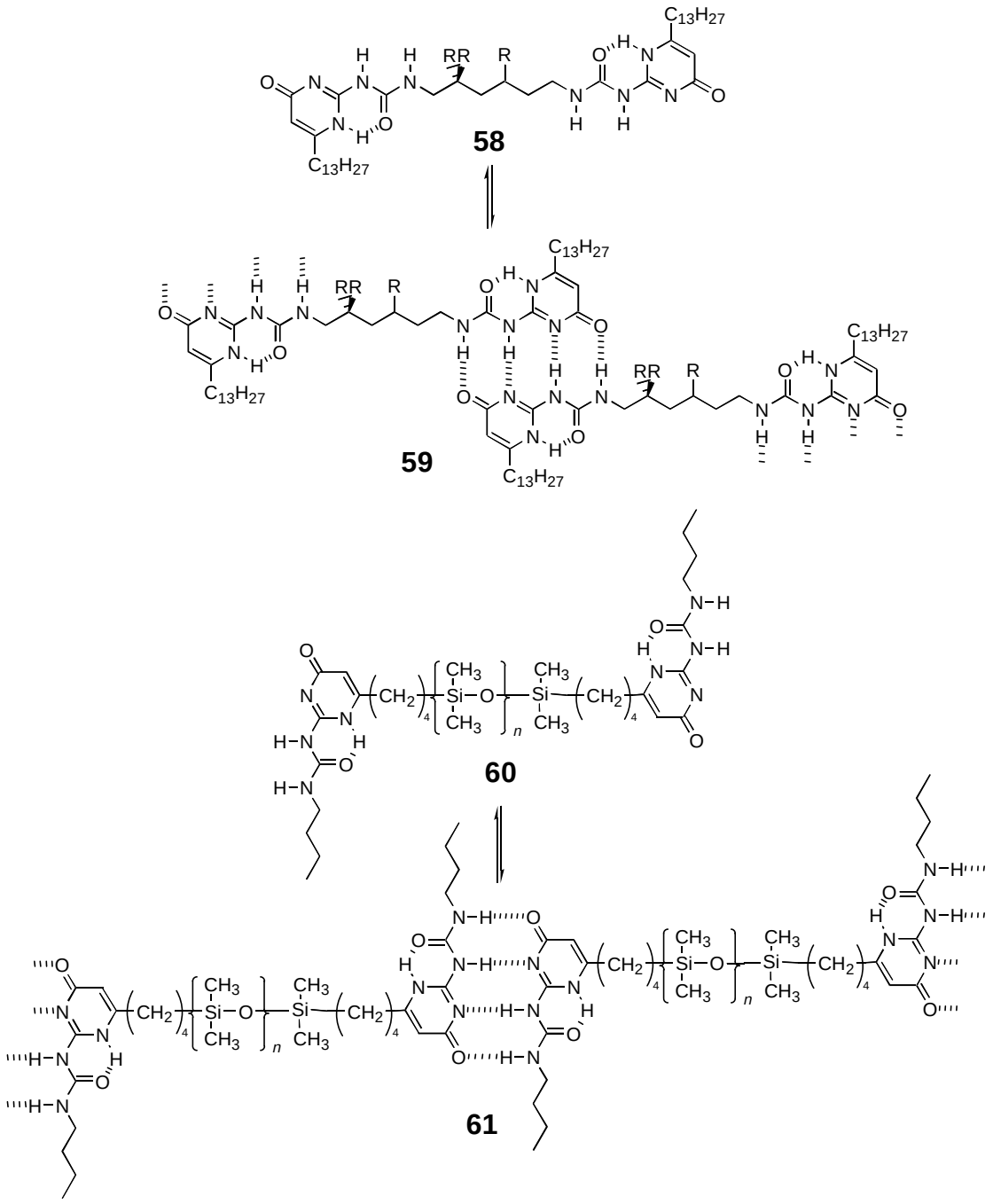

Figure 1.28. Self-assembly of supramolecular polymers **60** and **61**.[97,98]

1.4. Conclusions

By understanding the self-assembling phenomena occurring in biological systems (section 1.2), in the recent years chemists have made tremendous strides toward more

efficient construction of supramolecular structures. The extensive literature reviews described in the previous sections 1.3.1 and 1.3.2 demonstrate the feasibility of the molecular self-assembling approaches (the "bottom up" approaches) to generate well-defined structures and this concept has been extended to synthesize supramolecular polymeric nanostructures of various types (section 1.3.3) for potential applications in material science.

1.5. Goals and Outline of This Thesis

The construction of pseudorotaxane structures, particularly the ones demonstrated by Stoddart and his coworkers, is an emerging topic of great interest due to its remarkable efficiency and selectivity and unique geometry which ultimately allows mechanically linked structures to be formed after successful "blocking reactions". To the best of our knowledge, however, little is exploited on synthesis of pseudorotaxane-based supramolecular polymeric structures such as novel polypseudorotaxanes, linear arrays, and dendrimers. Thus, our goal was to first understand the dynamics of pseudorotaxane formation between monomeric crown ethers of appropriate sizes, namely bis-*m*-phenyl-32-crown-10 (BMP32C10) and DB24C8 with either 4.4"-bispyridine salt derivatives or secondary ammonium salts. Secondly, it was to transfer the knowledge gained from the studies of the monomeric pseudorotaxane systems to the synthesis of supramolecular polymeric structures, which were characterized by using techniques available in polymer chemistry, depending on the size and nature of the nanostructures.

1.6. References

1)Lindsey, J. S. *New J. Chem.* **1991**, *15*, 153-180.

2)Whitesides, G. M.; Mathias, J. P.; Seto, C. T. *Science* **1991**, *254*, 1312-1319.

3)Lehn, J.-M. *Supramolecular Chemistry Concepts and Perspectives*; VCH: New York, 1995.

4)Philp, D.; Stoddart, J. F. *Angew. Chem. Int. Ed. Engl.* **1996**, *35*, 1154-1196.

5)Batten, S. R.; Robson, R. *Angew. Chem. Int. Ed.* **1998**, *37*, 1460-1494.

6)Reinhoudt, D. N.; Stoddart, J. F.; Ungaro, R. *Chem. Eur. J.* **1998**, *4*, 1349-1351.

7)de Mendoza, J. *Chem. Eur. J.* **1998**, *4*, 1373-1377.

8)Rebek, J., Jr. *Angew. Chem. Int. Ed. Engl.* **1990**, *29*, 245-255.

9)Vögtle, F. *Suparmolecular Chemistry*; John Wiley & Sons: New York, 1991.

10)Amabilino, D. B.; Stoddart, J. F. *Chem. Rev.* **1995**, *95*, 2715-2828.

11)Fyfe, M. C. T.; Stoddart, J. F. *Acc. Chem. Res.* **1997**, *30*, 393-401.

12)Harada, A.; Li, J.; Kamachi, M. *Nature* **1992**, *356*, 325-327.

13)Harada, A.; Li, K.; Kamachi, M. *Nature* **1994**, *370*, 126-128.

14)Klug, A. *Angew. Chem. Int. Ed. Engl.* **1983**, *22*, 565-582.

15)Whitesides, G. M.; Ismagilov, R. F. *Science* **1999**, *284*, 89-92.

16)Stryer, L. *Biochemistry*; Fourth Edition ed.; W. H. Freeman and Company: New York, 1995.

17)Petrucci, R. H. *General Chemistry: Principles and Modern Applications*; Fifth Edition ed.; Macmillan Publishing Company: New York, 1989.

18)Voet, D.; Voet, J. G. *Biochemistry*; Second Edition ed.; John Wiley & Sons, Inc.: New York, 1994.

19)Wang, Y.; Wei, B.; Wang, Q. *J. Crystallogr. Spectrosc. Res.* **1990**, *20*, 79-84.

20)Seto, C. T.; Whitesides, G. M. *J. Am. Chem. Soc.* **1993**, *115*, 905-916.

21)Mammen, M.; Simanek, E. E.; Whitesides, G. M. *J. Am. Chem. Soc.* **1996**, *118*, 12614-12623.

22)Mammen, M.; Shakhnovich, E. I.; Deutch, J. M.; Whitesides, G. M. *J. Org. Chem.* **1998**, *63*, 3821-3830.

23)Valdés, C.; Toledo, L. M.; Spitz, U.; Rebek, J., Jr. *Chem. Eur. J.* **1996**, *2*, 989-991.

24)Kang, J.; Santamaría, J.; Hilmersson, G.; Rebek, J., Jr. *J. Am. Chem. Soc.* **1998**, *120*, 7389-7390.

25)Szabo, T.; Hilmersson, G.; Rebek, J., Jr. *J. Am. Chem. Soc.* **1998**, *120*, 6193-6194.

26)Tokunaga, Y.; Rudkevich, D. M.; Santamaría, J.; Hilmersson, G.; Rebek, J., Jr. *Chem. Eur. J.* **1998**, *4*, 1449-1457.

27)Marsh, A.; Silvestri, M.; Lehn, J.-M. *J. Chem. Soc., Chem. Commun.* **1996**, 1527-1528.

28)Allwood, B. L.; Spencer, N.; Shahriari-Zavareh, H.; Stoddart, J. F.; Williams, D. J. *J. Chem. Soc., Chem. Commun.* **1987**, 1064-1066.

29)Allwood, B. L.; Shahriari-Zavareh, H.; Stoddart, J. F.; Williams, D. J. *J. Chem. Soc., Chem. Commun.* **1987**, 1058-1061.

30)Ashton, P. R.; Philp, D.; Reddington, M. V.; Slawin, A. M. Z.; Spencer, N.; Stoddart, J. F.; Williams, D. J. *J. Chem. Soc., Chem. Commun.* **1991**, 1680-1683.

31)Amabilino, D. B.; Ashton, P. R.; Balzani, V.; Brown, C. L.; Credi, A.; Fréchet, J. M. J.; Leon, J. W.; Raymo, F. M.; Spencer, N.; Stoddart, J. F.; Venturi, M. *J. Am. Chem. Soc.* **1996**, *118*, 12012-12020.

32)Asakawa, M.; Ashton, P. R.; Ballardini, R.; Balzani, V.; Beloharadský, M.; Gandolfi, T.; Kocian, O.; Prodi, L.; Raymo, F. M.; Stoddart, J. F.; Venturi, M. *J. Am. Chem. Soc.* **1997**, *119*, 302-310.

33)Raymo, F. M.; Houk, K. N.; Stoddart, J. F. *J. Am. Chem. Soc.* **1998**, *120*, 9318-9322.

34)Ashton, P. R.; Baxter, I.; Cantrill, S. J.; Fyfe, M. C. T.; Glink, P. T.; Stoddart, J. F.; White, A. J. P.; Williams, D. J. *Angew. Chem. Int. Ed.* **1998**, *37*, 1294-1297.

35)Ashton, P. R.; Fyfe, M. C. T.; Martínez-Díaz, M.-V.; Menzer, S.; Schiavo, C.; Stoddart, J. F.; White, A. J. P.; Williams, D. J. *Chem. Eur. J.* **1998**, *4*, 1523-1534.

36)Martínez-Díaz, M.-V.; Spencer, N.; Stoddart, J. F. *Angew. Chem. Int. Ed. Engl.* **1997**, *36*, 1904-1907.

37)Fyfe, M. C. T.; Glink, P. T.; Menzer, S.; Stoddart, J. F.; White, A. J. P.; Williams, D. J. *Angew. Chem. Int. Ed. Engl.* **1997**, *36*, 2068-2070.

38)Ashton, P. R.; Ballardini, R.; Balzani, V.; Baxter, I.; Credi, A.; Fyfe, M. C. T.; Gandolfi, M. T.; Gómez-López, M.; Martínez-Díaz, M.-V.; Piersanti, A.; Spencer, N.; Stoddart, J. F.; Venturi, M.; White, A. J. P.; Williams, D. J. *J. Am. Chem. Soc.* **1998**, *120*, 11932-11942.

39)Ashton, P. R.; Fyfe, M. C. T.; Glink, P. T.; Menzer, S.; Stoddart, J. F.; White, A. J. P.; Williams, D. J. *J. Am. Chem. Soc.* **1997**, *119*, 12514-12524.

40)Ashton, P. R.; Glink, P. T.; Stoddart, J. F.; Tasker, P. A.; White, A. J. P.; Williams, D. J. *Chem. Eur. J.* **1996**, *2*, 729-736.

41)Ashton, P. R.; Campbell, P. J.; Chrystal, E. J. T.; Glink, P. T.; Menzer, S.; Philp, D.; Spencer, N.; Stoddart, J. F.; Tasker, P. A.; Williams, D. J. *Angew. Chem. Int. Ed. Engl.* **1995**, *34*, 1865-1869.

42)Ashton, P. R.; Chrystal, E. J. T.; Glink, P. T.; Menzer, S.; Schiavo, C.; Stoddart, J. F.; Tasker, P. A.; Williams, D. J. *Angew. Chem. Int. Ed. Engl.* **1995**, *34*, 1869-1871.

43)Ashton, P. R.; Chrystal, E. J. T.; Glink, P. T.; Menzer, S.; Schiavo, C.; Spencer, N.; Stoddart, J. F.; Tasker, P. A.; White, A. J. P.; Williams, D. J. *Chem. Eur. J.* **1996**, *2*, 709-728.

44)Glink, P. T.; Schiavo, C.; Stoddart, J. F.; Williams, D. J. *J. Chem. Soc., Chem. Commun.* **1996**, 1483-1450.

45)Ashton, P. R.; Collins, A. N.; Fyfe, M. C. T.; Glink, P. T.; Menzer, S.; Stoddart, J. F.; Williams, D. J. *Angew. Chem. Int. Ed. Engl.* **1997**, *36*, 59-62.

46)Ashton, P. R.; Fyfe, M. C. T.; Hickingbottom, S.; Menzer, S.; Stoddart, J. F.; White, A. J. P.; Williams, D. J. *Chem. Eur. J.* **1998**, *4*, 577-589.

47)Ashton, P. R.; Glink, P. T.; Martínez-Díaz, M.-V.; Stoddart, J. F.; White, A. J. P.; Williams, D. J. *Angew. Chem. Int. Ed. Engl.* **1996**, *35*, 1930-1933.

48)Ashton, P. R.; Ballardini, R.; Balzani, V.; Fyfe, M. C. T.; Gandolfi, M. T.; Martínez-Díaz, M.-V.; Morosini, M.; Schiavo, C.; Shibata, K.; Stoddart, J. F.; White, A. J. P.; Williams, D. J. *Chem. Eur. J.* **1998**, *4*, 2332-2341.

49)Ashton, P. R.; Baxter, I.; Fyfe, M. C. T.; Raymo, F.; Spencer, N.; Stoddart, J. F.; White, A. J. P.; Williams, D. J. *J. Am. Chem. Soc.* **1998**, *120*, 2297-2307.

50)Ashton, P. R.; Ballardini, R.; Balzani, V.; Gómez-López, M.; Lawrence, S. E.; Martínez-Díaz, V.; Montalti, M.; Piersanti, A.; Prodi, L.; Stoddart, J. F.; Williams, D. J. *J. Am. Chem. Soc.* **1997**, *119*, 10641-10651.

51)Loeb, S. J.; Wisner, J. A. *J. Chem. Soc., Chem. Commun.* **1998**, 2757-2758.

52)Loeb, S.; Wisner, J. *Angew. Chem. Int. Ed.* **1998**, *37*, 2838-2840.

53)Hamilton, D. G.; Sanders, J. K. M.; Davis, J. E.; Clegg, W.; Teat, S. J. *J. Chem. Soc., Chem. Commun.* **1997**, 897-898.

54)Hamilton, D. G.; Davies, J. E.; Prodi, L.; Sanders, J. K. M. *Chem. Eur. J.* **1998**, *4*, 608-620.

55)Amabilino, D. S.; Dietrich-Buchecker, C. O.; Livoreil, A.; Pérez-García, L.; Sauvage, J.-P.; Stoddart, J. F. *J. Am. Chem. Soc.* **1996**, *118*, 3905-3913.

56)Baumann, F.; Livoreil, A.; Kaim, W.; Sauvage, J.-P. *J. Chem. Soc., Chem. Commun.* **1997**, 35-36.

57)Cárdenas, D. J.; Gaviña, P.; Sauvage, J.-P. *J. Chem. Soc., Chem. Commun.* **1996**, 1915-1916.

58)Collin, J.-P.; Gaviña, P.; Sauvage, J.-P. *J. Chem. Soc., Chem. Commun.* **1996**, 2005-2006.

59)Carina, R., F.; Deitrich-Buchecker, C.; Sauvage, J.-P. *J. Am. Chem. Soc.* **1996**, *118*, 9110-9116.

60)Dietrich-Buchecker, C. O.; Sauvage, J.-P.; Armaroli, N.; Ceroni, P.; Balzani, V. *Angew. Chem. Int. Ed. Engl.* **1996**, *35*, 1119-1121.

61)Kusukawa, T.; Fujita, M. *J. Am. Chem. Soc.* **1999**, *121*, 1397-1398.

62)Fujita, M.; Yu, S.-Y.; Kusukawa, T.; Funaki, H.; Ogura, K.; Yamaguchi, K. *Angew. Chem. Int. Ed.* **1998**, *37*, 2082-2085.

63)Müller, C.; Whiteford, J. A.; Stang, P. J. *J. Am. Chem. Soc.* **1998**, *120*, 9827-9837.

64)Stang, P. J.; Olenyuk, B. *Angew. Chem. Int. Ed. Engl.* **1996**, *35*, 732-736.

65)Stang, P. J.; Persky, N. E.; Manna, J. *J. Am. Chem. Soc.* **1997**, *119*, 4777-4778.

66)Stang, P. J. *Chem. Eur. J.* **1998**, *4*, 19-27.

67)Manna, J.; Kuehl, C. J.; Whiteford, J. A.; Stang, P. J.; Muddiman, D. C.; Hofstadler, S. A.; Smith, R. D. *J. Am. Chem. Soc.* **1997**, *119*, 11611-11619.

68)Whang, D.; Park, K.-M.; Heo, J.; Ashton, P. R.; Kim, K. *J. Am. Chem. Soc.* **1998**, *120*, 4899-4900.

69)Zeng, F.; Zimmerman, S. C. *Chem. Rev.* **1997**, *97*, 1681-1712.

70)Zimmerman, S. C.; Zeng, F.; Reichert, D. E. C.; Kolotuchin, S. V. *Science* **1996**, *271*, 1095-1098.

71)Vollmer, M. S.; Clark, T. D.; Steinem, C.; Ghadiri, M. R. *Angew. Chem. Int. Ed.* **1999**, *38*, 1598-1601.

72)Rapaport, H.; Kim, H. S.; Kjaer, K.; Howes, P. B.; Cohen, S.; Als-Nielsen, J.; Ghadiri, M. R.; Leiserowitz, L.; Lahav, M. *J. Am. Chem. Soc.* **1999**, *121*, 1186-1191.

73)Ghadiri, M. R.; Kobayashi, K.; Granja, J. R.; Chadha, R. K.; McRee, D. E. *Angew. Chem. Int. Ed. Engl.* **1995**, *34*, 93-95.

74)Hartgerink, J. D.; Clark, T. D.; Ghadiri, M. R. *Chem. Eur. J.* **1997**, *4*, 1367-1372.

75)Clark, T. D.; Kobayashi, K.; Ghadiri, M. R. *Chem. Eur. J.* **1998**, *5*, 782-792.

76)Gong, C.; Gibson, H. W. *Angew. Chem. Int. Ed.* **1998**, *37*, 310-314.

77)Gong, C.; Balanda, P. B.; Gibson, H. W. *Macromolecules* **1998**, *31*, 5278-5289.

78)Owen, G. J.; Hodge, P. *J. Chem. Soc., Chem. Commun.* **1997**, 11-12.

79)Mason, P. E.; Parsons, I. W.; Tolley, M. S. *Polymer* **1998**, *39*, 3981-3991.

80)Mason, P. E.; Parsons, I. W.; Tolley, M. S. *Angew. Chem. Int. Ed. Engl.* **1996**, *35*, 2238-2241.

81)Mason, P. E.; Bryant, W. S.; Gibson, H. W. *Macromolecules* **1999**, *32*, 1559-1569.

82)Swager, T. M. *Acc. Chem. Res.* **1998**, *31*, 201-207.

83)Zhu, S. S.; Carroll, P. J.; Swager, T. M. *J. Am. Chem. Soc.* **1996**, *118*, 8713-8714.

84)Baxter, P. N. W.; Lehn, J.-M.; Baum, G.; Fenske, D. *Chem. Eur. J.* **1999**, *5*, 102-112.

85)Baxter, P. N. W.; Lehn, J.-M.; Kneisel, B. O.; Baum, G.; Fenske, D. *Chem. Eur. J.* **1999**, *5*, 113-120.

86)Lehn, J.-M. *Angew. Chem. Int. Ed. Engl.* **1990**, *29*, 1304-1319.

87)Lehn, J.-M. *Makromol. Chem., Macromol. Symp.* **1993**, *69*, 1-17.

88)Kimizuka, N.; Fujikawa, S.; Kuwahara, H.; Kunitake, T.; Marsh, A.; Lehn, J.-M. *J. Chem. Soc., Chem. Commun.* **1995**, 2103-2104.

89)Kihara, H.; Kato, T.; Uryu, T.; Fréchet, J. M. J. *Chem. Mater.* **1996**, *8*, 961-968.

90)Kawakami, T.; Kato, T. *Macromolecules* **1998**, *31*, 4475-4479.

91)Kato, T.; Ihata, O.; Ujiie, S.; Tokita, M.; Watanabe, J. *Macromolecules* **1998**, *31*, 3551-3555.

92)Kato, K.; Kubota, Y.; Uryu, T.; Ujiie, S. *Angew. Chem. Int. Ed. Engl.* **1997**, *36*, 1617-1618.

93)Kato, T.; Kihara, H.; Ujiie, S.; Uryu, T.; Fréchet, J. M. J. *Macromolecules* **1996**, *29*, 8734-8739.

94)Kato, T.; Fréchet, J. M. J. *Macromol. Symp.* **1995**, *98*, 311-326.

95)St. Pourcain, C. B.; Griffin, A. C. *Macromolecules* **1995**, *28*, 4116.

96)Folmer, B. J. B.; Cavini, E.; Sijbesma, R. P.; Meijer, E. W. *J. Chem. Soc., Chem. Commun.* **1998**, 1847-1848.

97)Ky Hirschberg, J. H. K.; Beijer, F. H.; van Aert, H. A.; Magusin, P. C. M. M.; Rint P. Sijbesma, R. P.; Meijer, E. W. *Macromolecules* **1999**, *32*, 2696 -2705.

98)Sijbesma, R. P.; Beijer, F. H.; Brunsveld, L.; Folmer, B. J. B.; Hirschberg, J. J. K. K.; Lange, R. F. M.; Lowe, J. K. L.; Meijer, E. W. *Science* **1997**, *278*, 1601-1604.